Chapter 4

Optical Fibre Long-Period Gratings Functionalised with Nano-Assembled Thin Films: Approaches to Chemical Sensing

Sergiy Korposh, Stephen James, Ralph Tatam and Seung-Woo Lee

Additional information is available at the end of the chapter

http://dx.doi.org/10.5772/52935

1. Introduction

Optical techniques are considered as powerful tools for the development of chemical and biological sensors, covering a wide range of applications including bio-chemical and food analysis, and environmental and industrial monitoring [1, 2, 3]. Optical fibre sensors, as a result of their advantages such as high sensitivity, compactness, remote measurement and multiplexing capabilities, have attracted a great deal of attention for the development of refractometers and chemical sensors [4, 5, 6]. Refractometers and chemical sensors based on optical fibre gratings, both fibre Bragg gratings (FBGs) and long period gratings (LPGs), have been extensively employed for refractive index measurements and monitoring associate chemical processes since they offer wavelength-encoded information, which overcomes the referencing issues associated with intensity based approaches.

FBG based approaches have exploited side polished [7] and thinned [8,9] optical fibres to expose the evanescent field of the mode propagating in the core of the fibre to the surrounding medium, such that the Bragg wavelength becomes sensitive to the surrounding refractive index. The response of such sensors is non-linear, with a maximum predicted sensitivity of approximately 200 nm/refractive index unit (RIU) for indices close to that of the cladding of the optical fibre [8]. Experimental investigation revealed a sensitivity of 70 nm/RIU with a corresponding resolution of order 10^{-4} RIU, assuming that the Bragg wavelength is measured with a resolution of 1 pm [9].

The effective refractive indices of the modes of the cladding of the optical fibre are inherently sensitive to the surrounding refractive index. Tilted fibre Bragg gratings (TFBGs) and LPGs allow the controlled, resonant coupling of light from the core of the optical fibre into cladding modes. The characteristics of the resonant coupling are modified by changes

in the surrounding refractive index, affording the ability to form refractive index sensors without altering the geometry of the optical fibre.

TFBGs facilitate the coupling of the propagating core mode to backward propagating cladding modes. As the coupling wavelength and efficiencies are dependent upon the properties of the cladding modes, the resonance features in the TFBG transmission spectrum exhibit sensitivity to surrounding refractive index [10,11]. Analysis of the transmission spectrum facilitates measurements with resolution of 10^{-4} RIU [11]. The use of thin film coatings of refractive index higher than that of the cladding on both polished FBGs and TFBGS has been shown to allow the RI range over which the devices show their highest sensitivity to the tuned to lower values [10,12,13].

LPGs promote coupling between the propagating core mode and co-propagating cladding modes, i.e. work as transmission gratings and are more attractive for practical applications as compared to FBGs, owing to lower cost of analytical instruments used to interrogate them. The high attenuation of the cladding modes results in the transmission spectrum of the fibre containing a series of attenuation bands centred at discrete wavelengths, each attenuation band corresponding to the coupling to a different cladding mode, as shown in Figure 1 [14].

The refractive index sensitivity of LPGs arises from the dependence of the phase matching condition upon the effective refractive index of the cladding modes that is governed by Equation 1 [14]:

$$\lambda_{(x)} = (n_{core} - n_{clad(x)})\Lambda \tag{1}$$

where $\lambda_{(x)}$ represents the wavelength at which the coupling occurs to the linear polarized (LP_{0x}) mode, n_{core} is the effective RI of the mode propagating in the core, $n_{clad(x)}$ is the effective RI of the LP_{0x} cladding mode, and Λ is the period of the grating.

The effective indices of the cladding modes are dependent upon the difference between the refractive index of the cladding and that of the medium surrounding the cladding. The central wavelengths of the attenuation bands thus show a dependence upon the refractive index of the medium surrounding the cladding, with the highest sensitivity being shown for surrounding refractive indices close to that of the cladding of the optical fibre, provided that the cladding has the higher refractive index [15]. For surrounding refractive indices higher than that of the cladding, the centre wavelengths of the resonance bands show a considerably reduced sensitivity [15].

The refractive index sensitivity of an LPG is dependent upon the order of the cladding mode that is coupled to, allowing the tuning of the sensitivity by appropriate choice of grating period, with 427.72, 203.18, 53.45, and 32.10 nm/RIU being reported for LPGs fabricated in single mode fibre (SMF) 28 with period 159, 238, 400, and 556 μm, respectively [16]. A further consideration is the geometry and composition of the fibre, with the sensitivity being shown to differ for step index and W profile fibres and a progressive three layered fibre [17]. New fibre geometries, such as photonic crystal fibres [18,19] and photonic band gap fibres [20]

have also been investigated for the measurement of the refractive index of a liquid that fills the air channels. LPGs in liquid filled solid-core photonic bandgap fibre have been shown to exhibit a sensitivity of 17,900 nm/RIU to changes in the RI of the liquid [21], but the requirement to fill the fibre with the liquid of interest may limit application as a refractometer.

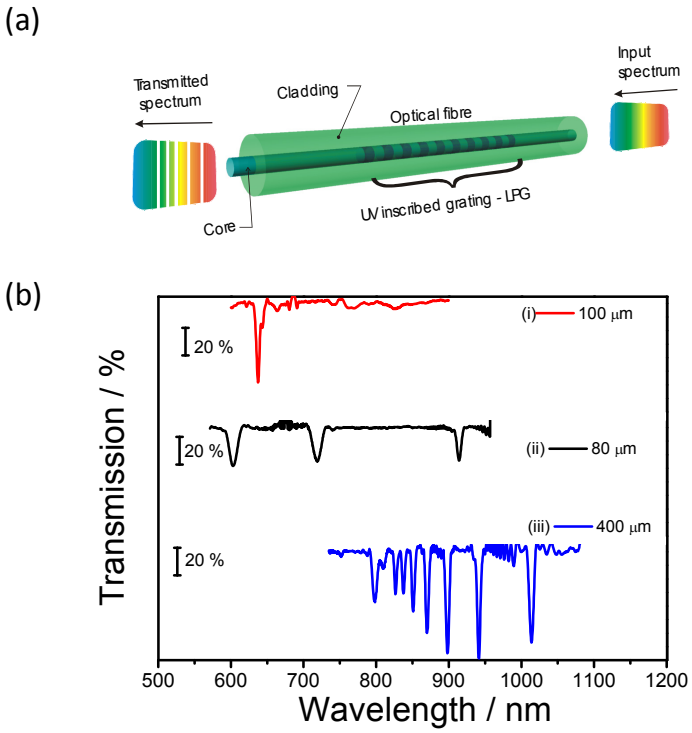

Figure 1. (a) Schematic illustration of the LPG structure and (b) transmission spectra of LPGs with different grating periods fabricated in an optical fibre of cut-off wavelength 670 nm (Fibrecore sm700): (i) 80 μm, (ii) 100 μm, and (iii) 400 μm [5].

In order to improve the sensitivity of the LPGs written in standard optical fibre configurations to surrounding RI, approaches such as tapering the fibre [22] or etching the cladding [23,24] have been investigated. Tapering the fibre to a diameter of 25 μm allowed the demonstration of an LPG with a sensitivity of 715 nm/RIU [22]. Etching the cladding of a section of standard single mode fibre containing an LPG from 125 μm to approximately 100 μm produced a sensitivity gain of 5 [25], while the etching an arc induced LPG to a diameter of 37 μm allowed the demonstration of a sensitivity of order 20,000 nm/RIU [26]. Approaches that require the processing of the fibre, such as polishing, etching and tapering, produce significant enhancements in sensitivity, but at the cost of requiring careful packaging to compensate for the inevitable reduction in the mechanical integrity of the device.

The deposition of thin film overlays, of thickness on the order of 200 nm, of materials of refractive index higher than that of the cladding has also been investigated for the

enhancement of refractive index sensitivity [25,26]. It has been shown previously experimentally and theoretically [27,28] that the effective indices of the cladding modes, and thus the central wavelengths of the core-cladding mode coupling bands of LPGs, show a high sensitivity to the optical thickness of high refractive index coatings when the coating's optical thickness is such that one of the low order cladding modes is phase matched to a mode of the waveguide formed by the coating. This is termed the *mode transition region*, in which the cladding modes are reorganized, with each mode taking on the characteristics (effective index and electric field profile) of its adjacent lower order cladding mode [29]. The output from a numerical model of the influence of coating thickness on the effective indices of the cladding modes of an optical fibre is plotted in Figure 2, showing clearly the mode transition region.

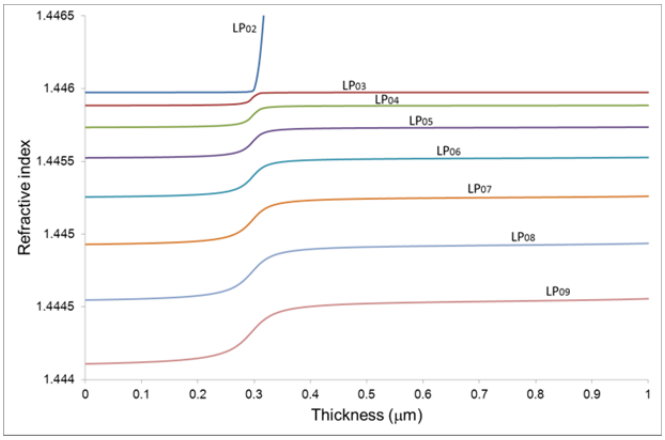

Figure 2. Plot of the effective refractive indices of the first 9 cladding modes as a function of the thickness of an overlay of refractive index. The model assumed values for the core and cladding refractive indices of 1.4496 and 1.446 respectively, a core radius of 3.5 μm, and that the refractive index of the overlay material was 1.57.

Biasing the optical thickness of the coating such that the LPG is operating in the *mode transition region* enhances the sensitivity of the cladding mode effective indices and thus the resonance wavelengths to the surrounding refractive index. A theoretical analysis explored the optimization of the refractive index sensitivity by selecting grating period, coating thickness and refractive index, predicting a sensitivity of 5980 nm/RIU [29].

In addition, the combination of optical fibers and nanomaterials provides a prospect for the fabrication of chemical sensors with high sensitivity and that offer specific response to targeted chemical species [30,31]. Achieving the coating thickness that provides optimized sensitivity requires control on the nm scale, which is why many reports have exploited the Langmuir Blodgett (LB) and layer-by-layer (LbL) electrostatic self assembly (ESA) coating deposition techniques, where a multilayer coating is deposited with each layer having a thickness of order 1 nm. Based on this principle, sensors for organic vapors, metal ions, humidity, organic solvents and biological materials have been reported [32, 33, 34]. Similarly

to surface plasmon resonance (SPR) devices, LPG sensors can provide highly precise analytical information about adsorption and desorption processes associated with the RI and thickness of the sensing layer. For instance, the sensitivity of LPG sensors is in the same order of magnitude as SPR sensors, showing a sensitivity of ca. 1 nM for antigen–antibody reactions. An advantage of the LPG over SPR lies in the ability to fabricate a cheap and portable device that can be applied in various analytical situations.

The influence of the period of the LPG on the sensitivity of the mode coupling to perturbations such as changes in surrounding RI can be understood with reference to the phase matching condition, equation (1). Using the weakly guided approximation it is possible to determine the effective indices of the modes of the core and cladding, and, using equation 1, to generate a family of phase matching curves that describe the variation of the resonant wavelength with period of the LPG, an example is shown in Figure 3. It can be seen that the phase matching condition for each cladding mode contains a turning point. The resonance features in the LPG spectrum exhibit their highest sensitivity to external perturbations near the phase matching turning point. The response of the transmission spectrum of an LPG operating near the phase matching turning point external perturbation, in this case changes to the optical thickness of a coating deposited onto the optical fibre, are illustrated in Figure 4. In Figure 4a, the grating period is such that phase matching to the LP_{020} cladding mode is satisfied, but it is not possible to couple to the LP_{021} cladding mode, with a resulting LPG transmission spectrum of the form shown in Figure 4b. Changes in the optical thickness (product of the geometrical thickness and refractive index) of the coating cause an increase in the effective refractive index of the cladding modes, and the phase matching curves change accordingly, as illustrated in Figure 4c, resulting in the development of a resonance band corresponding to coupling to the LP_{021} cladding mode, and a small blue shift in the central wavelength of the LP_{020} resonance band, Figure 4d. Further increases in the optical thickness of the coating result in the further development of the LP_{021} resonance band, which subsequently splits into two bands, the so called dual resonance, Figures 4f and 4h. The small gradient of the phase matching curve at the phase matching turning point results in the LP_{021} resonance band exhibiting much higher sensitivity than the LP_{020} resonance band for this grating period. Thus the sensitivity of coated LPG sensors can be optimised by appropriate choice of the optical thickness of the coating and period of the grating to ensure that the LPG operates at both the mode transition region and the phase matching turning point.

Recently, LPG fibre sensors with porous coatings have attracted a lot of interest. For instance, a sol-gel film of SnO_2 of thickness of order 200 nm was deposited onto to an LPG, facilitating the demonstration of an ethanol gas sensor. The porosity and high RI of the coating material resulted in the LPG spectrum exhibiting a response to the diffusion of ethanol gas into the coating and the authors predicted that an optimized sensor would exhibit a detection limit of 100 ppb. Sol-gel coatings of SiO_2 and TiO_2 have been deposited onto LPGs, revealing a gain of 2 in the sensitivity to external RI, with the higher index TiO_2 coating offering the larger response (up to 1067.15 nm/RIU). The authors noted that the higher the index and thickness of the coating the more pronounced was the enhancement in LPG sensitivity compared to the equivalent uncoated LPG [16].

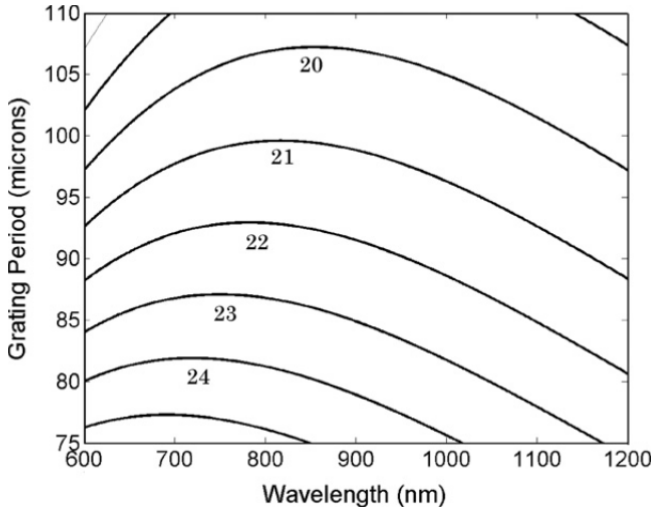

Figure 3. Phase matching curves for higher order cladding modes of an optical fibre of cut off wavelength 670 nm. The numbers refer to the order of the cladding mode.

Recently we have demonstrated a fibre optic refractive index sensor based on a long period grating (LPG) with a nano-assembled mesoporous coating of alternate layers of poly(allylamine hydrochloride) (PAH) and SiO_2 nanospheres [5, 6]. PAH/SiO_2 coatings of different thicknesses were deposited onto an LPG operating near its phase matching turning point in order to study the effect of the film thickness and porosity on sensor performance. The device showed a high sensitivity (1927 nm/RIU) to RI changes with a response time less than 2 sec over a wide RI range (1.3330–1.4906). The low refractive index of the mesoporous film, 1.20@633 nm, facilitates the measurement of external indices higher than that of the cladding, extending the range of operation of LPG based RI sensors. The ability of this device to monitor, in real time, RI changes during a dilution process was also demonstrated.

In this chapter we introduce a new approach to LPG based chemical sensing. A novel 2 stage approach to the development of the sensor is explored. The first stage involves the deposition of the mesoporous coating onto the LPG operating near the phase matching turning point. In the second stage a functional material, chosen to be sensitive to the analyte of interest, is infused into the base mesoporous coating. The mesoporous coating consists of a multilayer film of SiO_2 nanoparticles (SiO_2 NPs) deposited using the LbL technique. The initially low RI of the mesoporous coating, 1.2@633 nm, is increased significantly by the chemical infusion, resulting in a large change in the LPG's transmission spectrum. The sensing of ammonia in aqueous solution was chosen to demonstrate the sensing principle. The operation of the sensor was characterised using two functional materials, tetrakis-(4-sulfophenyl)porphine (TSPP) and polyacrylic acid (PAA). TSPP is a porphine compound that changes its optical properties (absorbance and RI) in response to exposure to ammonia, while PAA has been employed as a functional compound ammonia binding [35]. In the case of the PAA it is assumed that direct biding of ammonia to the COOH moiety will change RI of the mesoporous coating, while in the case of TSPP its desorption will result on RI change.

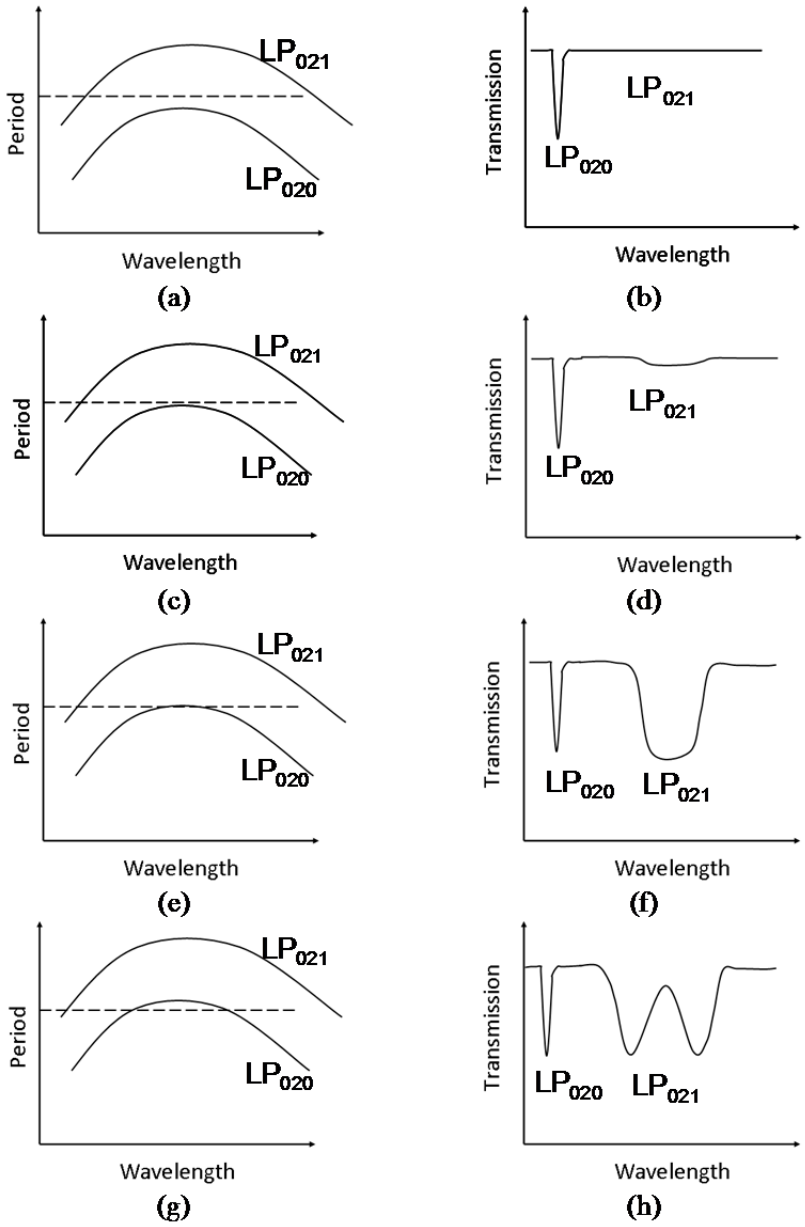

Figure 4. Optical features of the LP_{020} and LP_{021} cladding modes near the phase matching turning point. An increase in the effective index of the cladding modes, caused for example by an increase in the surrounding refractive index, or in the optical thickness of a coating deposited onto the fibre, cause the phase matching curves to move as shown, producing large changes in the coupling characteristics and transmission spectrum.

2. Sensor fabrication

Tetrakis-(4-sulfophenyl)porphine (TSPP, Mw = 934.99) was purchased from Tokyo Kasei, Japan. Poly(diallyldimethylammonium chloride) (PDDA, Mr = 200,000–350,000, 20% (w/w) in H2O; monomer Mw = 161.5 g mol−1), PAA_{25} (Mw: 250,000, 35 wt% in H_2O) and ammonia 30 wt% aqueous solution were purchased from Aldrich. A colloidal solution of silica nanoparticles (SiO_2 NPs), SNOWTEX 20L (40–50 nm), was purchased from Nissan Chemical. All chemicals were reagents of analytical grade, and used without further purification. Deionized pure water (18.3 MΩ·cm) was obtained by reverse osmosis followed by ion exchange and filtration in a Millipore-Q (Millipore, Direct-QTM).

A detailed description and reference to the optical properties of LPGs can be found elsewhere [5, 6, 36]. In this work, an LPG of length 30 mm with a period of 100 μm was fabricated in a single mode optical fibre (Fibercore SM750) with a cut-off wavelength of 670 nm using point-by-point UV writing process. The photosensitivity of the fibre was enhanced by pressurizing it in hydrogen for a period of 2 weeks at 150 bar at room temperature.

SiO_2 NPs were deposited onto the surface of the fibre using the LbL process, as illustrated in Figure 5a. As the LPG transmission spectrum is known to be sensitive to bending, for the film deposition process and ammonia detection experiments the optical fibre containing LPG was fixed within a special holder, as shown in Figure 5b, such that the section of the fibre containing the LPG was taut and straight throughout the experiments [36]. The detailed procedure of the deposition of the SiO_2 NPs onto the LPG and infusion of the TSPP compound has been previously reported [5]. Briefly, the section of the optical fibre containing LPG, with its surface treated such that it was terminated with OH groups, was alternately immersed into a 0.5 wt% solution containing a positively charged polymer, PDDA, and, after washing, into a 1 wt% solution containing the negatively charged SiO_2 NPs solution, each for 20 min. This process was repeated until the required coating thickness was achieved. When the required film thickness had been achieved (i.e. when the development of the second resonance band was observed with the fibre immersed into water), ca. after 10 deposition cycles, the coated fibre was immersed in a solution of TSPP or PAA as functional compound for 2 h, which was infused into the porous coating and provided the sensor with its specificity. Due to the electronegative sulfonic groups present in the TSPP compound, an electrostatic interaction occurs between TSPP and positively charged PDDA in the PDDA/SiO_2 film. On the other hand, PAA is usually considered as a promising sensor element for ammonia sensing, owing to the presence of free carboxylic function groups that lead to high affinity towards amine compounds [37]. After immersion into the TSPP and PAA solutions, the fibre was rinsed in distilled water, in order to remove physically adsorbed compounds, and dried by flushing with N_2 gas. The compounds remaining in the porous silica structure were bound to the surface of the polymer layer that coated each nanosphere. This effectively increased the available surface area for the compounds to bond to. The presence of functional chemical compounds increased the RI of the porous coating and resulted in a significant change in the LPG's transmission spectrum, consistent with previous observations for increasing the coating thickness [38]. All experiments have been conducted at 25°C and 50% of rH.

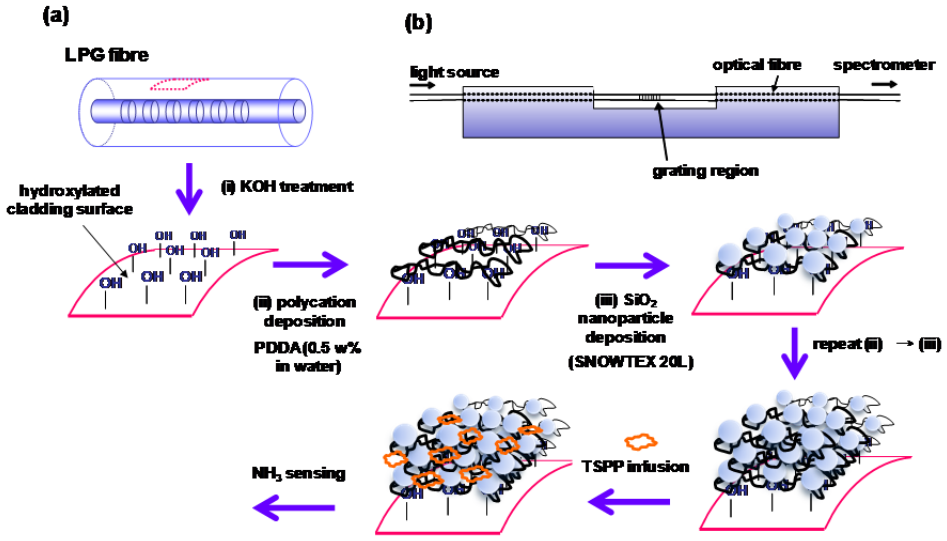

Figure 5. (a) Schematic illustration of the electrostatic self-assembly deposition process and (b) deposition cell with a fixed LPG fibre.

3. Mesoporous coating of long period gratings

Figures 6a and 6b show the surface morphology and cross-section of the 10-cycle (PDDA/SiO_2) layer, referred to as (PDDA/SiO_2)$_{10}$, on a quartz substrate, respectively. As can be seen, the (PDDA/SiO_2)$_{10}$ film has a uniform surface consisting of SiO_2 NPs with an average diameter of 45 nm (Figure 6a). The film thicknesses obtained after 1 and 10 cycles of the (PDDA/SiO_2) deposition process, determined from SEM cross-section measurements, are approximately 50±2 nm and 450±20 nm, respectively (Figures 6b and 6c). The pore size distribution of the (PDDA/SiO_2) film indicates a well-developed mesoporous structure with a mean pore radius of 12.5 nm and specific surface area of 50 $m^2\ g^{-1}$ [5].

The transmission spectrum of the 100 μm period LPG undergoes changes due to the alternate deposition of SiO_2 NPs, as shown in Figure 7, which influences the effective RI of the cladding mode, as described previously [5]. When the LPG was in the silica colloidal solution, the resonance feature (at ca. 640 nm) corresponding to coupling to the LP_{020} cladding mode exhibited a small blue wavelength shift of 8.5 nm. As the optical thickness of the coating increased, it became possible to couple energy to the LP_{021} mode, with the corresponding development of the resonance band at ca. 800 nm [5], at the phase matching turning point for that mode. However, because of the low RI (1.20) [39] of the porous silica coating, this resonance feature is not well developed in water and is not present in air for this coating thickness.

When an uncoated LPG fibre with a period of 100 μm is immersed into water (RI=1.323), a blue shift of the LP_{020} resonance band of 3 nm is observed. However, the sensitivity of the

LP_{020} resonance band is much improved by coating the LPG with a $(PDDA/SiO_2)_{10}$ film, showing a blue shift of 7 nm when the LPG was immersed in water, along with the appearance of the well pronounced second resonance band, LP_{021} (Figure 8a). This is attributed to the increase in sensitivity of the LPG to the surrounding RI [16], being of interest when measuring the RI of low concentration aqueous solutions. The response to the RI changes is fast (< 2 s) and stable, as indicated by the measurement of the transmitted power at the centre of the LP_{021} resonance (Figure 8b).

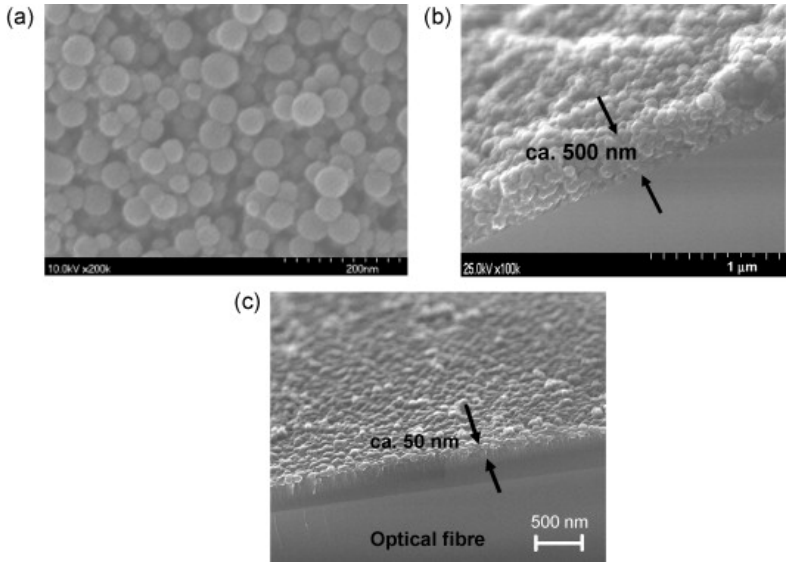

Figure 6. SEM images of the (a) surface morphology and (b) cross-section of the $(PDDA/SiO_2)_{10}$ film deposited on a quartz substrate before TSPP infusion; (c) cross section of a $(PDDA/SiO_2)_1$ film.

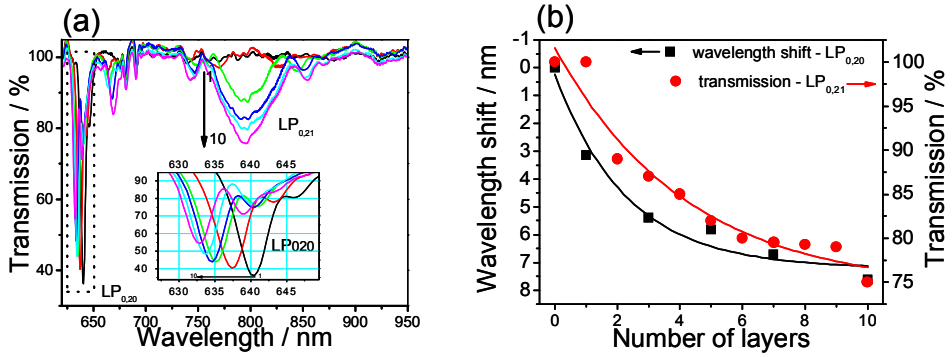

Figure 7. (a) Transmission spectra of the 100 μm period LPG in the colloidal SiO_2 solution in water after PDDA deposition (b) wavelength shifts and changes in transmission as a function of the number of deposition cycles for the LP_{020} and LP_{021} resonance bands, respectively; the curve is a guide to the eye only.

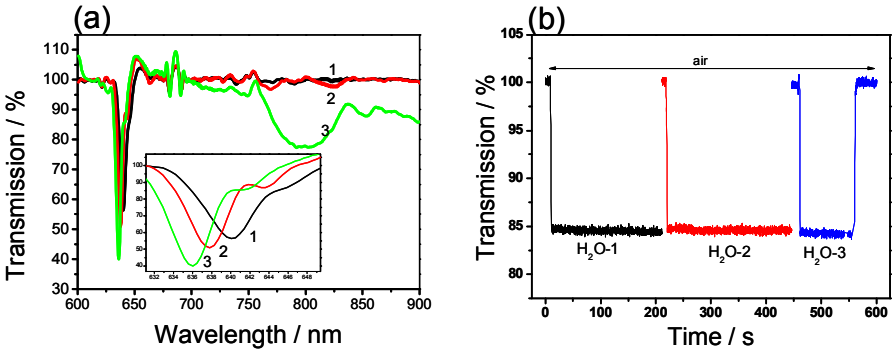

Figure 8. (a) Transmission spectra of the 100 μm period LPG under different conditions: black line, in air without coating; red line, in water without coating; green line, in water after deposition of the $(PDDA/SiO_2)_{10}$ film. (b) Dynamic changes of the transmission spectrum of the SiO_2 NP coated LPG measured at 800 nm in different phases from air to water.

The RI and film thickness of a 1-cycle PDDA/SiO_2 film, measured using ellipsometry, were 1.20 (at 633 nm) and 47±2 nm, respectively, which is in a good agreement with both the reported data for RI [39] and the thickness measured using SEM (see Figure 6b). It should be noted that dispersion of the RI in the wavelength range of 400–800 nm is negligible, with the RI value of 1.20±0.0001, and does not influence LPG sensor performance over the operational wavelength range of 600–900 nm. The deposition of the PDDA/SiO_2 layer was also monitored using the QCM technique and UV-vis spectroscopy (data not shown). A $(PDDA/SiO_2)_{10}$ film was deposited on two different QCM electrodes and a relative standard deviation of ±11% was obtained. The frequency linearly decreased as the number of the deposition cycles increased with average values of 1739±207 Hz and 30±10 Hz for the SiO_2 and PDDA layers, respectively. This corresponds to SiO_2 and PDDA masses of 1565 ng and 27 ng per each layer, respectively. The average thickness of the SiO_2 layer was 42±4 nm [36], which corresponds very well with the values determined using ellipsometry and SEM. A uniform PDDA/SiO_2 film was assembled on the quartz substrate, as revealed by the increase of the absorbance in the UV region with increment in the number of SiO_2 NP layers. The modulation observed in the absorption spectrum of the coated quartz slide was the result of the interference between light reflected from the front and rear surfaces of the coated slide, which introduces a channelled spectrum, the period and phase of which is dependent on the PDDA/SiO_2 film optical thickness. Thickness values of the PDDA/SiO_2 film deposited onto different substrates (quartz slab, silicon wafer and optical fibre) using a LbL method determined from SEM, QCM and ellipsometry measurements agreed well, within experimental error, regardless of the surface nature, indicating that the LbL method is an efficient tool for the deposition of uniform nano-thin films on different types of surfaces.

4. Employment of functional molecules and chemical sensing

The principle of operation of a coated LPG sensor operating at the phase matching turning point and applied to the detection of chemical components that can be bound through an

electrostatic interaction with PDDA in the mesopores of the film has been discussed previously [5]. The resonance bands (LP_{020} and LP_{021}) could be used for the detection of chemical components that can be bound through an electrostatic interaction with the cationic groups of PDDA in the mesopores of the film. When an LPG coated with a $(PDDA/SiO_2)_{10}$ film is immersed in a TSPP solution, the transmission spectrum undergoes significant changes. Figure 9a shows the transmission spectra recorded when the $(PDDA/SiO_2)_{10}$ film coated LPG was immersed in a 1 mM TSPP water solution. As the TSPP is infused into the film, the RI of the film increases (from 1.200 to ca. 1.540, measured using ellipsometry) and the phase matching condition for coupling to LP_{021} is satisfied. A broad single attenuation band is developed rapidly (within 60 s), which subsequently splits in two bands as the RI of the coating increases in response to the TSPP infusion. The required time to complete the binding between the TSPP and PDDA moieties is less than 600 s (Figure 9b). The observed response indicates a large increase in the optical thickness of the film, which is a result of the increase in the RI of the film, as the TSPP is infused into the porous structure and adsorbed to the PDDA moiety between SiO_2 NPs.

The evolution of the transmission spectrum of the SiO_2 coated LPG when immersed in the TSPP solution is shown in the grey scale plot shown in Figure 10, where the transmission is represented by white and black, corresponding to 100% and 0%, respectively. The dark line at around 635 nm, which originates at a wavelength of 640 nm in the uncoated LPG, represents the resonance band that corresponds to the first order coupling to the LP_{020} cladding mode. The discontinuity in the trace, at 60 s, occurred when the LPG was immersed in the solution and is a result of the LPG's sensitivity to the RI of the solution.

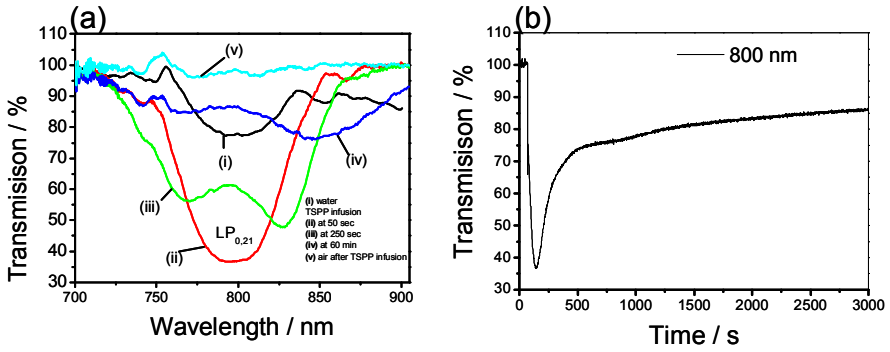

Figure 9. (a) Transmission spectra of the SiO_2 NP coated LPG and (b) the dynamic transmission change recorded at 800 nm when the SiO_2 NP coated LPG was immersed in a TSPP solution (1 mM in water).

In order to assess the sensitivity of the optical device, the $(PDDA/SiO_2)_{10}$ coated LPG was exposed to different concentrations of TSPP, and the results are shown in Figures 11a and 11b. The increase of the TSPP concentration from 10 to 1000 μM results in a decrease of the transmission measured at 800 nm, corresponding to the development of the LP_{021} cladding mode resonance. This is also accompanied by a blue shift of the LP_{020} resonance band, indicating the increase of the RI of the film. The response time of the sensor is observed to be

slower at lower TSPP concentrations. For 1 mM TSPP concentration, the increase in transmission at 800 nm, shown in Figures 11b, is attributed to the splitting of the fully developed LP_{021} cladding mode resonance into dual resonance bands.

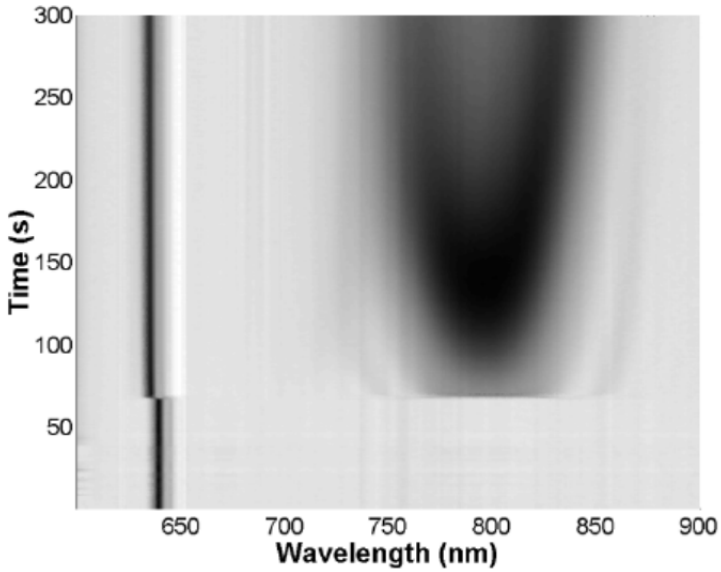

Figure 10. The evolution of the transmission spectrum of the SiO_2 NP coated LPG (period 100 μm), when immersed in an aqueous solution of TSPP (1 mM). The grey scale represents the measured transmission, with white corresponding to 100%, and black to 0%.

The ability to reuse the device was tested by removing the infused TSPP molecules from the film using an ammonia solution (ca. 1000 ppm). The spectrum was reverted to that observed for the $(PDDA/SiO_2)_{10}$ coated LPG before TSPP infusion. Subsequent immersion of the $(PDDA/SiO_2)_{10}$ coated LPG into the TSPP solutions allowed the results shown in Figure 11 to be reproduced.

A similar effect to that observed for the infusion of TSPP was observed when the $(PDDA/SiO_2)_{10}$ coated LPG was immersed into a PAA solution. The magnitude of the change, however, was smaller as compared to that induced by TSPP infusion, most plausibly being related to the lower RI of PAA (1.442) [40] as compared with that of TSPP (1.540) [5]. It should be noted that thickness of the $(PDDA/SiO_2)_{10}$ film was not changed on the infusion of the functional compounds, as revealed from SEM cross-sectional and ellipsometry measurements of the samples deposited onto the optical fibre before and after TSPP infusion (data not shown).

The infusion of the TSPP molecules into the $PDDA/SiO_2$ film deposited on a glass substrate was also investigated using UV-vis spectroscopy. Figure 12 shows the absorbance spectrum of the $PDDA/SiO_2$ film after infusion of the TSPP compound. As can be seen from Figure 12,

the two Soret bands at wavelengths 419 and 482 nm, along with well-pronounced Q-band at 700 nm, are present, which indicates that the TSPP compound forms *J*-aggregates in the porous silica film [41,42]. It was previously confirmed that nano-assembled thin films with TSPP in *J*-aggregate state are particularly sensitive to ammonia gas [42]. In this work, mesoporous SiO_2 NPs films infused with TSPP were to be used to detect the presence of ammonia in aqueous solutions. In order to study the stability of the PDDA/SiO_2 films infused with TSPP in aqueous solutions, they were immersed into water several times, with the resultant changes in absorption spectra shown in Figure 12. The second Soret-band (482 nm) and Q-band (at 700 nm) disappeared when the film was immersed into water, accompanied by a decrease in the absorbance of the first Soret-band (419 nm), which indicates the partial removal of the adsorbed TSPP molecules from the film [42]. We can speculate that this phenomenon is a result of the cleavage of the *J*-aggregates of TSPP formed in the space between the SiO_2 NPs.

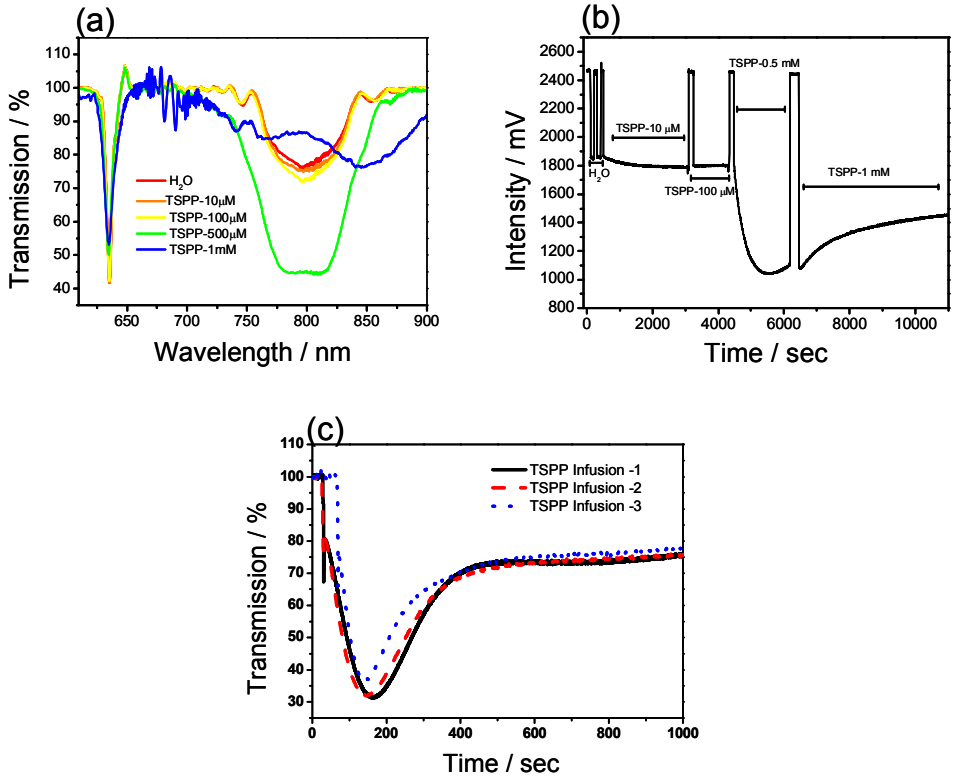

Figure 11. (a) Transmission spectra of the $(PDDA/SiO_2)_{10}$ coated LPG; (b) transmission change recorded at 800 nm in response to different concentrations of TSPP (from 10 μM to 1 mM in water) and (c) dynamic response to the three infusions of TSPP into the PDDA/SiO_2 porous film recorded at 800 nm; the infusion was conducted after complete removal of TSPP from the PDDA/SiO_2 using an NH_3 solution of concentration 1000 ppm.

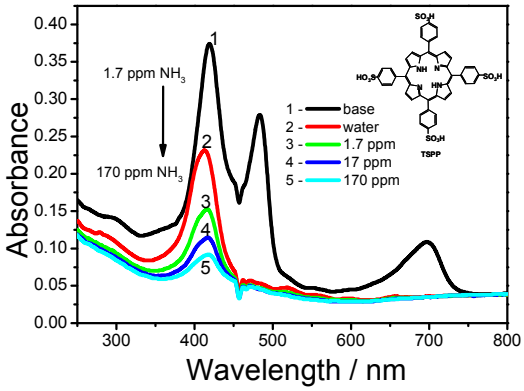

Figure 12. Absorption spectra of the $(PDDA/SiO_2)_{10}$ film infused with TSPP on a quartz plate: before immersion into H_2O (solid line) and after immersion into ammonia solutions of concentration from 0 ppm, 1.7 ppm, 17 ppm and 170 ppm (dashed lines); inset shows the structure of the TSPP.

The observed absorbance decrease reached a steady state after several immersions, indicating that only strongly bound TSPP molecules remained in the $PDDA/SiO_2$ porous film. Subsequently, immersion of the $PDDA/SiO_2$ film into aqueous solutions containing ammonia led to the further removal of TSPP from the film, resulting in a decrease of the absorbance at 419 nm in proportion to the ammonia concentration, as shown in Figure 12. The absorbance at 419 nm almost disappeared, at an ammonia concentration of 170 ppm.

The amount of TSPP infused inside the mesoporous film was estimated from QCM measurements to be 1135.6 ng (1.13 nmol). Consequently, considering the amount of adsorbed PDDA to be 250 ng (278 Hz for 10 cycles, 1.50 nmol as monomer unit of PDDA), the porous film contains sufficient binding sites for the infused TSPP molecules using the electrostatic interaction. When the QCM electrode that had been coated with a $(PDDA/SiO_2)_{10}$ film infused with TSPP was immersed into water and into ammonia, a similar trend to that measured using a UV-vis spectrophotometer was observed [36]. In particular, the frequency increased after each immersion into water (for 5 min) by up to a factor of 5, indicating the desorption of TSPP from the film; about 70% of the employed TSPP molecules were removed from the film [36]. Further immersion into water did not lead to a significant frequency change, suggesting that strongly bound TSPP (ca. 30% of the employed TSPP molecules) remained in the mesoporous film. When the film was exposed to ammonia solutions of different concentrations, further desorption of TSPP was observed and the total mass loss was 292 ng, indicating the almost complete removal of TSPP from the film [36]. Consequently, ca. 51 ng of TSPP remained in the film after ammonia treatment.

For ammonia detection, the sensing mechanism may be based upon changes in the RI of the coating resulting from chemically induced adsorption or desorption of the functional material to or from the mesoporous coating. Porphyrins have tetrapyrrole pigments [43] and their optical spectrum in the solid state is different to that in solution, due to the presence of

strong π–π interactions [43]. Interactions with some chemical species can produce further spectral changes, thus creating the possibility that they can be used in the development of optical sensor systems. For instance, exposure of TSPP that has sulfonic functional groups to ammonia leads to the modification of the absorption spectrum [42].

5. Ammonia sensing

The sensitivity to ammonia in water of an LPG coated with a $(PDDA/SiO_2)_{10}$ film that was infused with TSPP was characterized by sequential immersion of the coated LPG into ammonia solutions with different concentrations (0.1, 1, 5 and 10 ppm). The lower ammonia concentrations were prepared by dilution of the stock solution of 28 wt%. In order to assess the stability of the base line, the coated LPG was immersed several times into 150 μL of pure water. The decrease of attenuation of the second resonance band, LP_{021}, at 800 nm, indicates the partial removal of the adsorbed TSPP molecules as discussed above. The equilibrium state was achieved after several exposures into water. For the ammonia detection, the LPG fibre was exposed into a 150 μL ammonia solution of 0.1 ppm, followed by drying and immersion into ammonia solutions of 1, 5 and 10 ppm.

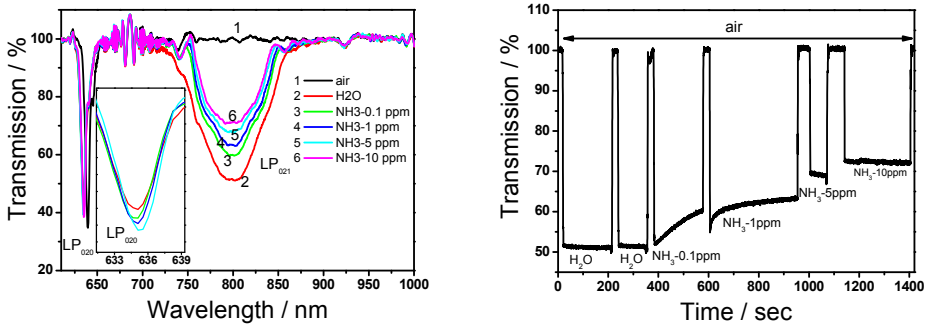

(a) (b)

Figure 13. (a) Transmission spectra of the LPG coated with a TSPP infused $(PDDA/SiO_2)_{10}$ film due to immersion into water and into ammonia solutions of different concentrations: "H_2O", LPG exposed into water; "air", LPG in air after drying with N_2 gas; "NH_3 x ppm", LPG exposed into a x ppm ammonia solution, where x = 0.1, 1, 5 and 10. (b) Dynamic response to water and ammonia solutions (0.1, 1, 5 and 10 ppm) recorded at 800 nm; LP_{020} and LP_{021} are labelling the linear polarized 020 and 021 modes, respectively.

The response of the transmission spectrum to varying concentration of ammonia is shown in Figure 13a. The dynamic response of the sensor was assessed by monitoring the transmission at the centre of the LP_{021} resonance band at 800 nm. The response is shown in Figure 13b, where "air" region and "H_2O" and "NH_3" regions correspond to the transmission recorded at 800 nm after drying the LPG and exposing the devise into water and ammonium solutions, respectively. After repeating the process of immersion in water and drying 4 times, the recorded spectrum was stable, demonstrating the robustness and

stability of the employed molecules in aqueous environments (H_2O regions indicated in Figure 13). On immersion in 1 ppm and 5 ppm ammonia solutions, the transmission measured at 800 nm increases. The transmission when the coated LPG was immersed in a 10 ppm ammonia solution exhibits a further increase, reaching a steady state within 100 s, as shown in Figure 13b. The resonance feature corresponding to coupling to the LP_{020} cladding mode exhibits additional small red shifts of 0.5 and 1.5 nm when subsequently immersed in solutions of 1 ppm and 10 ppm ammonia concentration, respectively, along with decreases in amplitude, as shown in Figure 13a. The limit of detection (LOD) for the 100 μm period LPG coated with a $(PDDA/SiO_2)_{10}$ film that was infused with TSPP was 0.14 ppm and 2.5 ppm when transmission and wavelength shift were measured respectively. The LOD was derived from the calibration curve and the following equation [36, 44].

$$LOD=3\cdot\sigma/m \tag{2}$$

where σ is the standard uncertainty obtained as a symmetric rectangular probability [45]; m is the slope of the calibration curve. The sensing mechanism postulated is based upon the UV-vis spectrometer, QCM and LPG fibre measurements, and can be illustrated using Figure 14. As mentioned previously, while most of TSPP molecules form J-aggregates in the PDDA/SiO2 film, some of the molecules are present in monomeric forms, as shown in Figure 14a, which may be easily sulfonated into species with neutral ($TSPP^{4-}$) and protonated (H_2TSPP^{2-}) pyrrole rings in water. As can be concluded from UV-vis measurements, on immersion of the TSPP-infused $PDDA/SiO_2$ film into water, most of J-aggregated TSPP molecules are removed from the mesopores between SiO_2 NPs, Figure 12. This indicates that the intermolecular interaction between J-aggregates of TSPP can be easily broken in water. However, some strongly bond TSPP compounds remained in the porous film. Figure 14b shows the chemical reactions involved in the interaction of ammonia with the $TSPP^{4-}$ and H_2TSPP^{2-} monomers. The electrostatic interaction between TSPP and PDDA is disturbed by the formation of ammonium ions and this causes the further desorption of the TSPP compound from the $PDDA/SiO_2$ film and consequently a decrease in the refractive index of the film.

It is important to consider the influence of the pH of the ammonia solutions on the sensor response, as the electrostatic interaction between TSPP and PDDA can be disturbed by OH^- ions in solution. To check this, the pH of the ammonia solutions used in this work were measured using a compact pH meter (B-211, Horiba), showing 7.3, 7.3 and 7.6 for 0.1, 1, and 10 ppm solutions, respectively. Thus, the molar concentration of NH_3 and OH^- is estimated to be 0.58, 5.8 and 58 mM for NH_3 and 0.25, 0.25 and 50 nM for OH^-, respectively. These data reveal that the concentration of OH^- does not have a significant role and the sensing mechanism is mainly based on the basicity of ammonia, as shown in Figure 14b. The cross sensitivity of the LPG sensor was tested using ethanol and methanol aqueous solutions. There was no measurable response of the sensor at the concentration levels similar to those tested for ammonia (0.1, 1, 10 and 100 ppm) indicating high selectivity of the sensor device to ammonia over those analytes. At much higher concentrations (10,000 ppm), however, blue-shift of the LP_{020} band and decrease in transmission at 800 nm was registered, which can be ascribed to the change of the bulk RI of the solution [6].

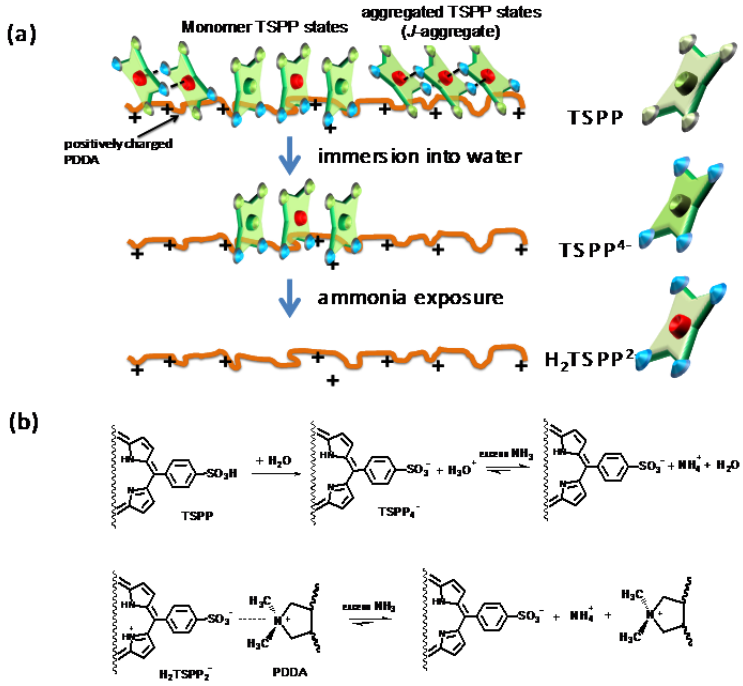

Figure 14. Schematic illustration of the sensing mechanism.

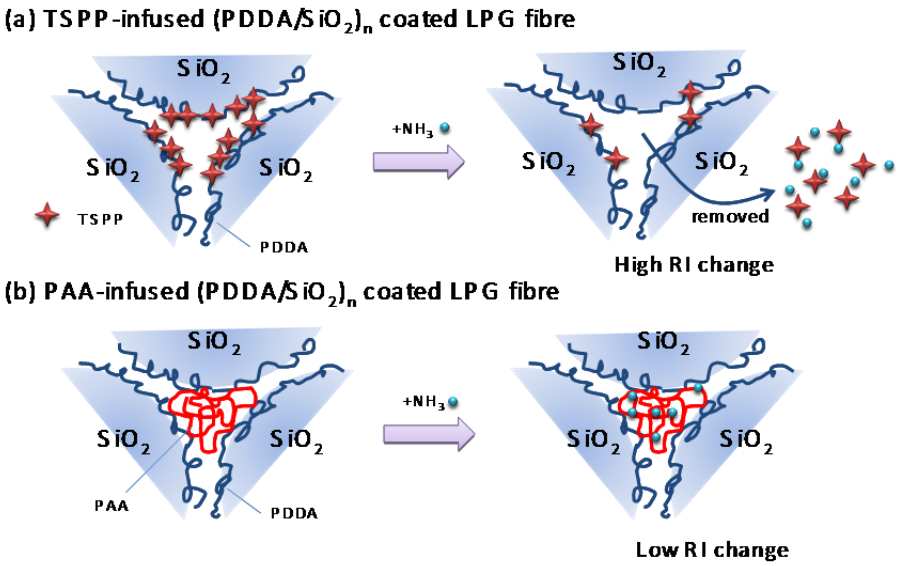

Scheme 1. Schematic illustration of the ammonia sensing mechanism for the LPG fibres modified with (a) TSPP-infused PDDA/SiO_2 and (b) PAA-infused PDDA/SiO_2 films.

The assessment of the cross sensitivity to other amine containing compounds is in progress. When compared with other ammonia optical sensors [46] the developed LPG device shows similar detection levels to coulorometric [47] and absorption spectroscopy [48] devices. In particular, the current LPG optical fibre sensor modified with a mesoporous thin film offers unique advantages such as versatile chemical infusion of various chemicals into the mesopores, fast response time owing to the easy analyte penetration and robustness. In addition, due to unique properties of the optical fibre such as biocompatibility, multiplexing, small size, immunity to electromagnetic interference and possibility to work in harsh environment, a cost effective, portable sensor system can be produced. To further elucidate the sensing principle of the LPG sensor, the response of a $(PDDA/SiO_2)_{10}$ coated LPG and of a PAA-infused $(PDDA/SiO_2)_{10}$ coated LPG was further examined. There was no change when the $(PDDA/SiO_2)_{10}$ and PAA infused $(PDDA/SiO_2)_{10}$ coated LPGs were exposed to ammonia solutions which have similar values of RI, 1.3329, from 1 ppm to 100 ppm concentrations as measured using a portable refractometer (R-5000, Atago). Thus, no change in sensor signal was recorded in the $(PDDA/SiO_2)_{10}$ coated LPG. On the other hand, higher affinity to ammonia based on the acid-base interaction is expected in the PAA-infused $(PDDA/SiO_2)_{10}$ coated LPG [39]. However, no response to ammonia was observed. This indicates that the adsorption of ammonia in small molecular size results in a small RI change. Consequently, the selective desorption of the functional compound with a high RI from the mesoporous film results in a significant increase in the device sensitivity, as shown in Scheme 1. This measurement principle can be further explored for a different set of analyte-functional compound pair including biological analytes expanding the application range of the proposed LPG device.

6. Device repeatability

It was observed that, if the sensor was repeatedly exposed to a certain concentration of ammonia following a washing and drying cycle, the response was not reproducible, in that on each subsequent exposure to ammonia the extinction of the band was further reduced, as shown in Figure 13. The extinction of the band still changes in time and the effect saturates with the increase of the ammonia concentration, in the way indicated in Figure 13 b. The linear dependence of the sensor response upon the ammonia concentration indicates that magnitude of the change on each exposure is the same; thus proposed device can be employed for measurements of the cumulative exposure to ammonia. However, after a number of repeated exposures, with the number being dependent on the concentration of the ammonia solution to which the device was exposed, the sensitivity was exhausted, and exposure to the ammonia solution would produce a spectrum equivalent to that obtained after deposition of the porous film, but before TSPP infusion [5]. It was found that the TSPP compound could be infused into the porous film again by the exposure of the LPG to a 1 mM solution of TSPP (step (vii) in Figure 5). The reproducibility of the device was tested by the exposure of the LPG coated with the TSPP infused $(PDDA/SiO_2)_{10}$ film to an ammonia solution of concentration >1000 ppm (concentration chosen to ensure that the TSPP was completely desorbed from the PDDA/SiO2 film), followed by washing with pure water and

immersion in a 1 mM TSPP solution in order to regenerate the original film properties [5], Figure 11c. The procedure was repeated 5 times and the same behaviour and resulting LPG transmission spectrum were obtained after each reinfusion process. It should be noted that ammonia measurements were conducted 3 times at each concentration. These results indicate that highly reproducible measurements can be conducted by employing TSPP reinfusion step.

7. Summary

The response of the transmission spectrum of an LPG of period 100 μm to the deposition of a multilayer film of SiO_2 NPs and the subsequent infusion of a porphyrin into the porous coating has been characterized. The infusion of the functional materials, chosen to be sensitive to the analyte of interest, into the base mesoporous coating was reported. Two possible sensing mechanisms have been exploited, based upon changes in the refractive index of the coating resulting from (1) chemically induced RI changes of the mesoporous coating at the adsorption of the analyte to the functional material, namely PAA and (2) chemically induced desorption of the functional material, namely TSPP, from the mesoporous coating. The operation of the device as a re-useable ammonia sensor with a minimum detection level of 0.14 ppm and a response time of approximately 100 s exploiting desorption sensing mechanism has been reported. On the other hand, the ammonia adsorption to the carboxylic functional groups of the PAA resulted in a small RI change and low sensitivity to analyte. The film thicknesses and functional material infusion time employed in this work have been determined empirically, as the calculation of the RI of the porous coating infused with TSPP and immersed in water would be highly complex. Operation of the system at the point of coincidence of the mode transition region and phase matching turning point for films of larger/smaller thickness could be achieved by decreasing/increasing the quantity of the function dye infused into the film, and this may influence the minimum detectable concentration and sensitivity. Such issues are currently under investigation. Advantages of the proposed method lie in the ability to control functionality of the coating by, for instance, choosing different matrix polymers that extend the class of the detectable analytes. Additionally, infusion of different types of functional compounds would allow the detection of different chemicals using a similar principle of operation. Future work is planned to demonstrate the current system for sensing a variety of chemical and biological compounds and for gas sensing.

Author details

Sergiy Korposh and Seung-Woo Lee*
Graduate School of Environmental Engineering, the University of Kitakyushu, 1-1 Hibikino, Wakamatsu-ku, Kitakyushu, Japan

Stephen James and Ralph Tatam
School of Engineering, Cranfield University, Cranfield, Bedford, UK

* Corresponding Author

Acknowledgement

This work was supported by the Regional Innovation Cluster Program of the Ministry of Education, Culture, Sports, Science and Technology (MEXT), Japan and partly by the Ministry of Knowledge Economy (MKE, Republic of Korea) via the Fundamental R&D Program for Core Technology of Materials. The authors from Cranfield are grateful to the Engineering and Physical Sciences Research Council, EPSRC, UK for funding under grants EP/D506654/1 and GR/T09149/01.

8. References

[1] Tsuda H, Urabe K. Characterization of long-period grating refractive index sensors and their applications. Sensors 2009; 9 4559-4571.

[2] Libish T M, Linesh J, Biswas P, Bandyopadhyay S, Dasgupta K, Radhakrishnan P, Fiber Optic Long Period Grating Based Sensor for Coconut Oil Adulteration Detection. Sensors & Transducers Journal 2010; 114 102-111.

[3] James S W, Tatam R P. Optical fibre long-period grating sensors: characteristics and application. Measurement Science and Technology 2003; 14 R49-R61.

[4] Martinez-Rios A, Monzon-Hernandez D, Torres-Gomez I. Highly sensitive cladding-etched arc-induced long-period fiber gratings for refractive index sensing. Optics Communications 2010; 283 958-962.

[5] Korposh S, James S W, Lee S-W, Topliss S M, Cheung S C, Batty W J, Tatam R P. Fiber optic long period grating sensors with a nanoassembled mesoporous film of SiO2 nanoparticles. Optics Express 2010; 18 13227-13238.

[6] Korposh S, James S W, Tatam R P, S-W Lee. Refractive index sensitivity of fibre optic long period gratings coated with SiO2 nanoparticle mesoporous thin films. Meas. Sci. Tech. 2011; 22 075208s.

[7] Schroeder K, Ecke W, Mueller R, Willsch R, Andreev A A. A fibre Bragg grating refractometer. Measurement Science and Technology 2001; 12 757-764.

[8] Asseh A, Sandgren S, Åhlfeldt H, Sahlgren B, Stubbe R, Edwall G. Fiber optical bragg grating refractometer. Fiber and Integrated Optics 1998; 17(1) 51-62.

[9] Iadicicco A, Campopiano S, Cutolo A, Giordano M, Cusano A. Self temperature referenced refractive index sensor by non-uniform thinned fiber Bragg gratings. Sensors and Actuators, B: Chemical 2006; 120 231–237.

[10] Laffon G, Ferdinand P. Tilted short-period fibre-Bragg-grating-induced coupling to cladding modes for accurate refractometry. Measurement Science and Technology 2001; 12 765-770.

[11] Buggy S J, Chehura E, James S W, Tatam R P. Optical fibre grating refractometers for resin cure monitoring. Journal of Optics A: Pure and Applied Optics 2007; 9 S60-S65.

[12] Paladino D, Cusano A, Pilla P, Campopiano S, Caucheteur C and Mégret P. Spectral behavior in nano-coated tilted fiber Bragg gratings: Effect of thickness and external refractive index. IEEE Photonics Technology Letters 2007; 19 2051–2053.

[13] Caucheteur C, Paladino D, Pilla P, Cutolo A, Campopiano S, Giordano M, Cusano A, Mégret P. External refractive index sensitivity of weakly tilted fiber Bragg gratings with different coating thicknesses. IEEE Sensors Journal 2008; 8 1330-1336.

[14] V. Bhatia V, Vengsarkar A M. Optical fibre long-period grating sensors. Optics Letters 1996; 21 692-694.

[15] Shi Q, Kuhlmey B T. Optimization of photonic bandgap fiber long period grating refractive-index sensors. Optics Communications 2009; 282 4723-4728.

[16] Davies E, Viitala R, Salomäki M, Areva S, Zhang L, Bennion I. Sol-gel derived coating applied to long-period gratings for enhanced refractive index sensing properties. Journal of Optics A: Pure and Applied Optics 2009; 11 art. no. 015501.

[17] Allsop T, Webb D J, Bennion I. A comparison of the sensing characteristics of long period gratings written in three different types of fiber. Optical Fiber Technology 2003; 9 210-223.

[18] Yu X, Shum P, Ren G B, Ngo N Q. Photonic crystal fibers with high index infiltrations for refractive index sensing. Optics Communications 2008; 281 4555-4559.

[19] Zhu Y, He Z, Kaňka J, Du H. Numerical analysis of refractive index sensitivity of long-period gratings in photonic crystal fiber. Sensors and Actuators, B: Chemical 2008; 129 99-105.

[20] Shi Q, Kuhlmey B T. Optimization of photonic bandgap fiber long period grating refractive-index sensors. Optics Communications 2009; 282 4723-4728.

[21] Rees N D, James S W, Tatam R P, Ashwell G J. Optical fiber long-period gratings with Langmuir- Blodgett thin-film overlays. Optics Letters 2002; 27 686-688.

[22] Allsop T, Floreani F, Jedrzejewski K P, Marques P V S, Romero R, Webb D J, Bennion I. Spectral characteristics of tapered LPG device as a sensing element for refractive index and temperature. Journal of Lightwave Technology 2006; 24 870-878.

[23] Iadicicco A, Campopiano S, Giordano M, Cusano A. Spectral behavior in thinned long period gratings: effects of fiber diameter on refractive index sensitivity. Applied Optics 2007; 46 6945-6952.

[24] Martinez-Rios A, Monzon-Hernandez D, Torres-Gomez I. Highly sensitive cladding-etched arc-induced long-period fiber gratings for refractive index sensing. Optics Communications 2010; 283 958-962.

[25] Ishaq I M, Quintela A, James S W, Ashwell G J, Lopez-Higuera J M, Tatam R P. Modification of the refractive index response of long period gratings using thin film overlays. Sensors and Actuators, B: Chemical 2005; 107 738-741.

[26] Smietana M, Korwin-Pawlowski M L, Bock W J, Pickrell G R, Szmidt J. Refractive index sensing of fiber optic long-period grating structures coated with a plasma deposited diamond-like carbon thin film. Measurement Science and Technology 2008; 19 art. no. 085301.

[27] Rees N D, James S W, Tatam R P, Ashwell G J. Optical fiber long-period gratings with Langmuir- Blodgett thin-film overlays. Optics Letters 2002; 27 686-688.

[28] Cusano A, Iadicicco A, Pilla P, Contessa L, Campopiano S, Cutolo A, Giordano M. Cladding mode reorganization in high-refractive-index-coated long-period gratings: effects on the refractive-index sensitivity. Opt. Lett. 2005; 30 2536-8.
[29] Yang J, Yang L, Xu C-Q, Li Y. Optimization of cladding-structure-modified long-period-grating refractive-index sensors. Journal of Lightwave Technology 2007; 25 372-380.
[30] Del Villar I, Achaerandio M, Matias I R, Arregui F J. Deposition of overlays by electrostatic self assembly in long-period fibre gratings. Opt. Lett. 2005; 30 720-722.
[31] Del Villar I, Matias I R, Arregui F J. Influence on cladding mode distribution of overlay deposition on long period fiber gratings. J. Opt. Soc. Am. A 2006; 23 651-658.
[32] Cheung S C, Topliss S M, James S W, Tatam R P. Response of fibre optic long period gratings operating near the phase matching turning point to the deposition of nanostructured coatings. J. Opt. Soc. Am. B 2008; 25 897-902.
[33] Corres J M, Matias I R, del Villar I, Arregui F J. Design of pH sensors in long-period fiber gratings using polymeric nanocoatings. IEEE Sens. J. 2007; 7 455-463.
[34] Keith J, Hess L C, Spendel W U, Cox J A, Pacey G E. The investigation of the behavior of a long period grating sensor with a copper sensitive coating fabricated by layer-by-layer electrostatic adsorption. Tatanta 2006; 70 818-822.
[35] Schick G A, Schreiman I C, Wagner R W, Lindsey J S, Bocian D F. Spectroscopic characterization of porphyrin monolayer assemblies. J. Am. Chem. Soc. 1989; 111 1344-1350.
[36] Korposh S, Selyanchyn R, Yasukochi W, Lee S-W, James S, Tatam R. Optical fibre long period grating with a nanoporous coating formed from silica nanoparticles for ammonia sensing in water. Materials Chemistry and Physics 2012; 133 784-792.
[37] Lee S-W, Takahara N, Korposh S, Yang D-H, Toko K, Kunitake T. Nanoassembled thin film gas sensors. III. Sensitive detection of amine odors using TiO2/poly(acrylic acid) ultrathin film quartz crystal microbalance sensors. Anal. Chem., 2010; 82 2228-2236.
[38] Ye C C, James S W, Tatam R P. Simultaneous temperature and bend sensing with long-period fiber gratings. Optics Letters 2000; 25 1007-1009.
[39] Bravo J, Zhai L, Wu Z, Cohen R E, Rubner M F. Transparent superhydrophobic films based on silica nanoparticles. Langmuir 2007; 23 7293-7298.
[40] Currie E P K, Sieval A B, Fleer G J, Cohen Stuart M A. Polyacrylic acid brushes: Surface pressure and salt-induced swelling. Langmuir 2000; 16 8324-8333.
[41] Korposh S, Kodaira S, Batty W J, James S W, Lee S-W. Nano-assembled thin film gas sensor. II. An intrinsic high sensitive fibre optic sensor for ammonia detection. Sensor and Materials. 2009; 21(4) 1790-189.
[42] Korposh S O, Takahara N, Ramsden J J, Lee S-W, Kunitake T. Nano-assembled thin film gas sensors. I. Ammonia detection by a porphyrin-based multilayer film. J. Biol. Phys. Chem. 2006; 6 125-133.
[43] Kadis KM, Smith KM, Guilard R. The Porphyrin Handbook. vol. 11–20, 3500. Academic Press, 2003.
[44] Swartz ME, Krull IS. Analytical Method Development and Validation, Marcel Dekker, Inc.: NY USA; 1997.

[45] Rafael G, Possetti C, Kamikawachi R C, Muller M, Fabris J L. Metrological evaluation of optical fiber grating-based sensors: An approach towards the standardization. J. Lightwave Technology (OFS-21). (2011) 2167500, DOI 10.1109/JLT.2011.2167500.

[46] Timmer B, Olthuis W, Berg A. Ammonia sensors and their applications—a review. Sens. Act. B. 2005; 107 666-677.

[47] Yimit A, Itoh K, Murabayashi M. Detection of ammonia in the ppt range based on a composite optical waveguide pH sensor. Sens. Act. B. 2003; 88 239-245.

[48] Huszár H, Pogány A, Bozóki Z, Mohácsi Á, Horváth L, Szabó G. Ammonia monitoring at ppb level using photoacoustic spectroscopy for environmental application. Sens. Act. B. 2008; 134 1027-1033.